

## MIR status report: an experiment for the measurement of the dynamical Casimir effect

This article has been downloaded from IOPscience. Please scroll down to see the full text article.

2008 J. Phys. A: Math. Theor. 41 164024

(<http://iopscience.iop.org/1751-8121/41/16/164024>)

View [the table of contents for this issue](#), or go to the [journal homepage](#) for more

Download details:

IP Address: 171.66.16.148

The article was downloaded on 03/06/2010 at 06:44

Please note that [terms and conditions apply](#).

# MIR status report: an experiment for the measurement of the dynamical Casimir effect

A Agnesi<sup>1,2</sup>, C Braggio<sup>3</sup>, G Bressi<sup>2</sup>, G Carugno<sup>3</sup>, G Galeazzi<sup>4</sup>, F Pirzio<sup>1,2</sup>,  
G Reali<sup>1,2</sup>, G Ruoso<sup>4</sup> and D Zanello<sup>5</sup>

<sup>1</sup> Dipartimento di Elettronica, Università di Pavia, Via Ferrata 1, 27100 Pavia, Italy

<sup>2</sup> INFN—Sezione di Pavia, Via U. Bassi 6, 27100 Pavia, Italy

<sup>3</sup> INFN—Sezione di Padova, Via Marzolo 8, 35131 Padova, Italy

<sup>4</sup> INFN—Laboratori Nazionali di Legnaro, Viale dell'Università 2, 35020 Legnaro, Italy

<sup>5</sup> INFN—Sezione di Roma, P.le A. Moro 2, 00185 Roma, Italy

E-mail: [Giuseppe.Ruoso@lnl.infn.it](mailto:Giuseppe.Ruoso@lnl.infn.it)

Received 22 October 2007, in final form 22 January 2008

Published 9 April 2008

Online at [stacks.iop.org/JPhysA/41/164024](http://stacks.iop.org/JPhysA/41/164024)

## Abstract

In this paper, the status of the experiment MIR (motion induced radiation) is reported. This experiment aims at measuring for the first time the dynamical Casimir effect by using an effective motion of a wall of a superconducting microwave resonant cavity. Effective motion is produced by periodic illumination of a semiconductor slab by means of an ultra-high-frequency amplitude modulated laser.

PACS numbers: 12.20.Fv, 42.50.Dv, 13.40.-f

(Some figures in this article are in colour only in the electronic version)

## 1. Our approach to the dynamical Casimir effect

The study of the quantum vacuum has seen, in the recent years, an increase in the number of dedicated experiments, following the pioneering results of Lamoreaux on the Casimir effect [1]. The interest on this subject is motivated by the possibility of attaining a more cogent verification of quantum electrodynamics (QED), giving at the same time results in other fields of fundamental physics research. Casimir effect experiments can, for example, shed light onto the field of non-Newtonian forces at small separation [2], and experiments which sense optical properties of vacuum under external fields [3] are able to search for small mass particles. Some of us were part of a measurement of the Casimir effect in the plane parallel configuration [4], and after that result became interested in the Casimir effect in the presence of accelerated boundaries, which is best known as the dynamic Casimir effect [5]. In the first experiment, the action of the vacuum results in a force acting between two media. In the second we try to reveal directly the presence of a non-empty vacuum by using a specifically designed

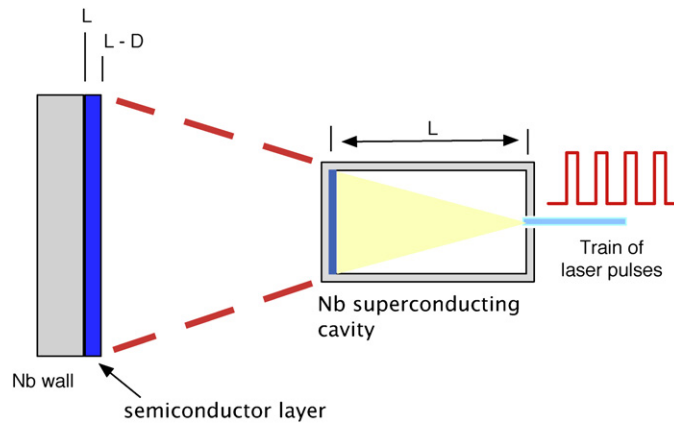


**Figure 1.** Principle of the experimental apparatus. On the left a larger view of the cavity end wall covered with a semiconductor layer is shown. Light will force the semiconductor to become reflecting, thus providing a change  $D$  of the cavity length  $L$ . Repeated pulses will produce harmonic oscillation.

device to amplify the virtual vacuum photons and produce real electromagnetic radiation. The ‘amplifier’ is nothing else than a boundary undergoing an oscillation, and hence radiates energy due to the dissipative action against the vacuum photons. The most obvious realization of this amplifier would be a single mirror moving with periodic motion at a frequency  $\Omega$ . Unfortunately, this system produces an undetectable number of photons  $N$ , approximately given by [6]  $N \sim \Omega T (v/c)^2$ , where  $T$  is the observation time,  $v$  is the maximum velocity and  $c$  is the speed of light. Using for the parameters the utmost values, i.e.  $\Omega \sim \text{GHz}$ ,  $(v/c) \sim 10^{-8}$  and observation time  $\sim 1$  s, the expected number of photons, generated at a frequency about  $\Omega$ , would be much less than 1. Such a small number of photons is undetectable, but it can be increased by realizing the moving boundary as part of a resonant cavity with the quality factor  $Q$ . If the resonant frequency  $\nu_r$  of the cavity fulfils the parametric resonance condition, i.e.  $2\nu_r = \Omega$ , the number of photons would then be  $QN$  [5, 7], which might be in the range of detectability. In our approach the cavity is a high- $Q$  superconducting niobium cavity where the moving boundary is realized by using a time variable mirror. Lozovik [8] and Yablonovitch [9] suggested the possibility of abrupt changes of the reflective properties of a semiconductor by using short intense laser pulses: following this idea we developed a scheme where a semiconductor switches from complete transparency to total reflection at a controlled frequency by using an amplitude-modulated laser beam [10]. This is depicted in figure 1. The semiconductor is illuminated by a train of laser pulses, with a repetition frequency twice the resonance frequency of the cavity. Each pulse has enough energy to produce in the semiconductor a plasma capable to reflect the electromagnetic radiation at frequency  $\nu_r$  [11]. If the recombination time of the semiconductor is short enough, at the end of each pulse the plasma will disappear. We will have achieved an effective motion of the boundary, which satisfies the parametric resonance condition. If the number of consecutive pulses is sufficient, a measurable signal will appear in the resonant cavity.

A complete parametrization of our set-up is currently under study by Dodonov [12]. In his calculation, all the parameters describing the apparatus are taken into account. The most critical ones are those regarding the behaviour of the semiconductor and the duration of the process of parametric amplification. The reference values used in the following come from Dodonov’s calculations.

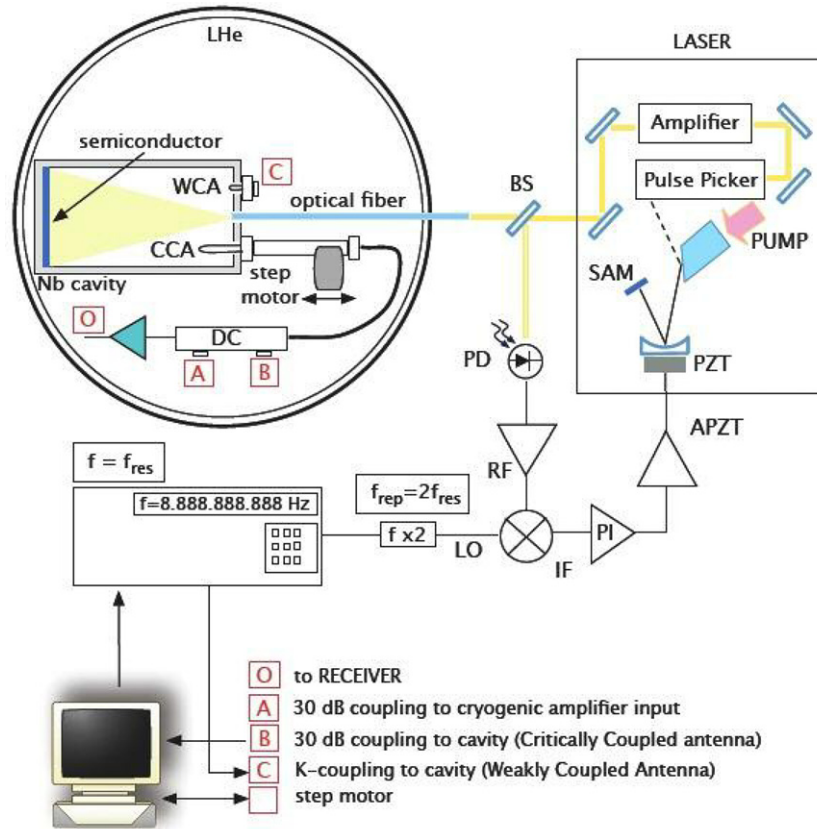


Figure 2. Schematic view of the experimental apparatus (see the text).

## 2. The apparatus

In figure 2, a schematic view of the apparatus is given. It is possible to identify a few blocks with the different elements of the system: a superconducting cavity with a semiconductor wall placed inside a liquid helium cryostat; a detection system for measuring a very small number of photons; the laser system; the data acquisition and general control of the apparatus. Details will now be given on the status of each part.

### 2.1. Resonant cavity and the cryogenic system

The core of the apparatus is a superconducting niobium cavity, with one face covered by the semiconductor layer. A picture of the cavity can be seen in figure 3. The cavity dimensions are  $9 \times 1 \times 8 \text{ cm}^3$  and has been optimized for a large dynamic Casimir effect signal [13]. One of the walls of the cavity can be removed and contains the groove for positioning the semiconductor slab. The cavity resonance frequency is 2.35 GHz and the  $Q$  value is in excess of  $10^6$  with the semiconductor inserted. The photons present in the cavity will be detected by a loop antenna coupled to a receiver chain. The antenna is inserted into the cavity by a hole and its position is controlled by a pair of computer-driven cryogenic motors. A feedback program optimizes the coupling by changing the antenna penetration and orientation with respect to

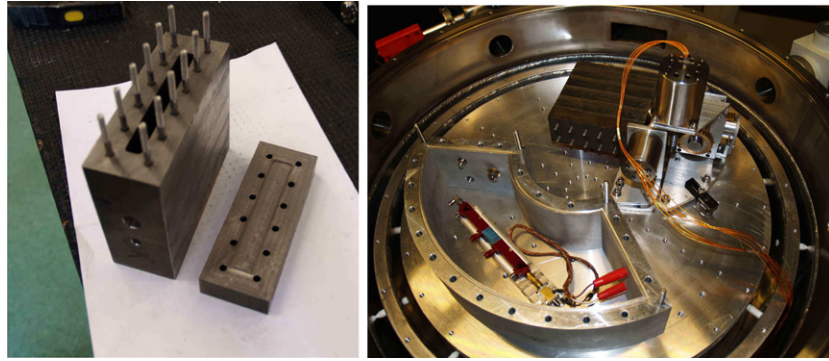


**Figure 3.** Left: picture of the resonant cavity. The cavity is open, the piece on the right is the top cover with the groove to hold the semiconductor. Right: the cavity inside the cryostat, equipped with motors to control the antenna position. The box on the lower left part of the picture on the right contains the cryogenic amplifier and a directional coupler. The box will be closed and filled with exchange helium gas to provide better cooling of the electronics.

the magnetic flux. All the components are kept inside a 50 L liquid helium cryostat. A duty period of 12 h is expected for a single filling of the cryostat, and working temperatures are in the range 1–8 K.

## 2.2. Semiconductor

There are two parameters about the semiconductor that are critical in the choice of the right material: the recombination time  $\tau$ , which should be of the order of 20 ps, and the mobility  $\mu$ , whose required value is  $\sim 1 \text{ m}^2 (\text{V s})^{-1}$ . After a long search we have discovered a procedure to realize semiconductors with the proper values: starting from bulk GaAs, having  $\tau \sim 1 \text{ ns}$  and  $\mu \sim 1 \text{ m}^2 (\text{V s})^{-1}$ , it is possible to reduce in a controlled way  $\tau$  while keeping  $\mu$  rather constant. This is done by irradiating the GaAs sample with fast neutrons (MeV energy range). The dose determines the recombination time, and we have found that a dose of  $\sim 10^{15}$  neutrons  $\text{cm}^{-2}$  results in a  $\tau \sim 20 \text{ ps}$ . Irradiation is performed at the laboratorio ENEA in Rome, and high sensitivity measurement (about 1 ps resolution) of the recombination time is performed with the THz pump and probe technique, at cryogenic temperature, by the group of Prof. Krotkus at the University of Vilnius. This measurement provides also an estimate of the sample mobility, which is roughly the bulk GaAs one as already shown by [14], i.e.  $\sim 1 \text{ m}^2 (\text{V s})^{-1}$  as requested.

## 2.3. Detection chain

The cavity photons are detected via a heterodyne scheme. The output signal from the antenna is first amplified by a cryogenic amplifier and then sent to the room temperature chain. After post-amplification the signal is down converted to 10.7 MHz frequency where it is again amplified and filtered around the cavity line width before being recorded with a fast sampling digital oscilloscope. In this scheme the final sensitivity is given, when optimized, by the noise temperature  $T_n$  of the first amplification stage. The measurement scheme for  $T_n$  is shown in figure 4. Using a heated  $50 \text{ } \Omega$  resistance and measuring the output power  $P$  of the chain for several resistance temperatures  $T_R$ , the noise temperature is obtained fitting the data with the function

$$P = k_b B G (T_R + T_n) \quad (1)$$

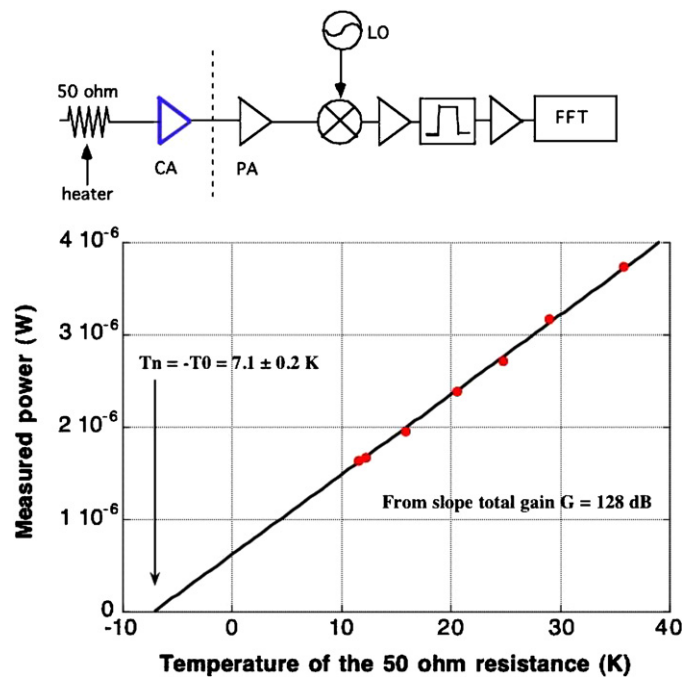


**Figure 4.** Noise temperature measurement. In the upper part the set-up and in the lower part the measured power versus temperature of the heated resistance superimposed with the fit. In the set-up: CA—cryogenic amplifier; PA—post amplifier; LO—local oscillator. The signal from the post amplifier is mixed with a local oscillator output and fed into a chain amplifier–band pass filter–amplifier. The output is analysed by a fast Fourier transform analyser (FFT).

where  $B$  is the bandwidth and  $G$  is the total gain of the receiver chain. We obtained  $T_n = 7.1 \pm 0.2$  K, with a total gain  $G = 128$  dB. The resulting sensitivity is 100 photons for a single measurement.

#### 2.4. Laser

The laser must satisfy very stringent parameters: a long enough train of pulses, each pulse must have more than  $100 \mu\text{J}$  energy, must be a few ps long and the distance between pulses about 200 ps (corresponding to an amplitude modulation of 5 GHz). We would also need wavelength tunability around 800 nm and frequency of modulation variable within 20 MHz. These parameters are not available in commercial laser systems, and for this reason the light source was realized in-house.

We built a Nd:YVO<sub>4</sub> laser generating a stable cw ( $\lambda = 1064$  nm) mode locking train of 4.4 ps pulses at 4.73 GHz, pumped by a 1 W laser diode emitting at 808 nm [15]. This source is injected onto a pulse picker system, which selects a number of consecutive pulses to be fed into an optical amplifier [16]. The number of pulses to be amplified is chosen by considering the ratio between the total energy available in the amplifier, presently about 500 mJ, and the minimum energy per pulse. After the pulse picker, the infrared radiation is frequency doubled and, using an optical parametric amplifier, converted into 800 nm radiation. The maximum energy attainable in the final stage is  $\sim 200$  mJ.

### 3. Expected sensitivity and background effects

The measurement procedure will be as follows: precise determination of the cavity resonance frequency  $\nu_r$  and tuning of the laser amplitude modulation rate exactly at  $2\nu_r$ . Sending the train of pulses to the semiconductor slab inside the cavity will produce a parametric amplification process with gain  $G_V$ . Since the minimum detectable number of photons for our detection chain is about 100, this means that a gain of about 100 must be reached to see the amplified vacuum photons. This value is within the capability of the apparatus. Actually, since the procedure can be repeated, even a lower gain can be tolerated. A precise evaluation of the gain will be performed once all the values of the various parameters will be fixed. The measurement of the gain will be the first task to be performed once the assembly of the complete set-up is finished, i.e. in the first half of 2008. This measurement will be done using a cavity preloaded with a known amount of energy, inserted using a weakly coupled antenna. The use of a preloaded cavity allows a larger dynamic response for the measurement scheme.

As for backgrounds, the presence of thermal photons is perhaps the largest effect one has to deal with to disentangle the contribution of the vacuum photons. The number of thermal photons  $N_T$  at equilibrium inside a resonant microwave cavity at the temperature  $T$  can be estimated using Planck formula as

$$N_T = \frac{1}{e^{\frac{h\nu}{k_B T}} - 1} \simeq \frac{k_B T}{h\nu} \quad (2)$$

where  $k_B$  is the Boltzmann constant,  $h$  is the Planck constant and  $\nu$  is the cavity resonance frequency. For example, at 4 K one expects a thermal contribution of 33 photons: these photons will be amplified as the half vacuum photons. The procedure for discrimination will be based on multiple measurements at different temperatures  $T_i$ . We plan measurements in the range 1–7 K. In the presence of a gain  $G_V$  larger than the minimum detectable number of photons, the discrimination of the vacuum photons from the thermal photons is independent of  $G_V$ , and it becomes possible if the  $\chi^2$  is large enough:

$$\chi^2 = \sum_i \frac{[(\frac{1}{2} + N_{T_i}) - N_{T_i}]^2}{\sigma_i^2}. \quad (3)$$

Assuming a Poissonian distribution,  $\sigma_i^2 = k_B T_i / h\nu$ , we get

$$\chi^2 = \frac{h\nu}{4k_B} \sum_i \frac{1}{T_i}. \quad (4)$$

If, for example, we perform measurements at the following temperatures  $T_i = \{1, 2, 3, 4, 5, 6, 7\}$  K, a probability for  $\chi^2$  less than  $5 \times 10^{-3}$  can be reached averaging about 240 values for each  $T_i$ . For a repetition rate of the train of laser pulses of one per minute, this can easily be done in a few days of data taking.

A number of other procedures are also under study to disentangle a real signal from a systematic effect. These include detuning of laser frequency out of the parametric resonance, variation of the thickness and recombination time of the semiconductor and possible new shapes of the resonant microwave cavity.

### Acknowledgments

The group wishes to thank all the people at the INFN Laboratori Nazionali di Legnaro and INFN Sezione di Padova who are helping in pursuing this goal, with a special remark to L Badan and E Berto for mechanics and cryogenics expertise and D Corti for the electronics. GR thanks F Della Valle for a critical reading of the manuscript.

**References**

- [1] Decca *et al* 2007 *Phys. Rev. D* **75** 077101  
Chen *et al* 2007 *Phys. Rev. B* **76** 035338  
For a review see Bordag M, Mohideen U and Mostepanenko V M 2001 *Phys. Rep.* **353** 1  
Lamoreaux S K 2005 *Rep. Prog. Phys.* **68** 201
- [2] Onofrio R 2006 *New J. Phys.* **8** 237
- [3] Zavattini E *et al* 2006 *Phys. Rev. Lett.* **96** 110406
- [4] Bressi G, Carugno G, Onofrio R and Ruoso G 2002 *Phys. Rev. Lett.* **88** 041804
- [5] Moore G T 1970 *J. Math. Phys.* **11** 2679  
Fulling S A and Davies P C W 1976 *Proc. R. Soc. Lond. A* **348** 393  
Schwinger J 1992 *Proc. Natl Acad. Sci. U S A.* **89** 4091  
Kardar M and Golestanian R 1999 *Rev. Mod. Phys.* **71** 1233  
Dodonov V V 2001 *Modern Nonlinear Optics (Adv. Chem. Phys. Ser., vol 119)* ed M W Evans (New York: Wiley) p 309
- [6] Jaekel M T, Lambrecht A and Reynaud S 2002 *Proc. of the Ninth Marcel Grossmann Meeting* ed V G Gurzadyan, R T Jantzen and R Ruffini (Singapore: World Scientific) p 1447
- [7] Lambrecht A, Jaekel M T and Reynaud S 1996 *Phys. Rev. Lett.* **77** 615  
Crocce M, Dalvit D A R and Mazzitelli F D 2001 *Phys. Rev. A* **64** 013808  
Schaller G, Schützhold R, Plunien G and Soff G 2002 *Phys. Rev. A* **66** 023812
- [8] Lozovik Yu E, Tsvetus V G and Vinograd E A 1995 *JETP Lett.* **61** 723  
Lozovik Yu E, Tsvetus V G and Vinograd E A 1995 *Phys. Scr.* **52** 184
- [9] Yablonovitch E 1989 *Phys. Rev. Lett.* **62** 1742
- [10] Braggio C, Bressi G, Carugno G, Del Noce C, Galeazzi G, Lombardi A, Palmieri A, Ruoso G and Zanello D 2005 *Europhys. Lett.* **70** 754
- [11] Braggio C *et al* 2004 *Rev. Sci. Instrum.* **75** 4967  
Braggio C *et al* 2007 *Phys. Lett. A* **363** 33
- [12] Dodonov V V and Dodonov A V 2006 *J. Phys. B: At. Mol. Opt. Phys.* **39** S749
- [13] Dodonov V V and Dodonov A V 2006 *J. Phys. A: Math. Gen.* **39** 6271
- [14] Foulon F *et al* 2000 *J. Appl. Phys.* **88** 3634
- [15] Agnesi A, Pirzio F, Tomaselli A, Reali G and Braggio C 2005 *Opt. Express* **13** 5302
- [16] Agnesi A, Carr L, Pirzio F, Scarpa D, Tomaselli A, Reali G, Vacchi C and Braggio C 2006 *Opt. Express* **14** 9244